

# Open-Set Object Detection Using Classification-free Object Proposal and Instance-level Contrastive Learning

Zhongxiang Zhou, Yifei Yang, Yue Wang, Rong Xiong

**Abstract**—Detecting both known and unknown objects is a fundamental skill for robot manipulation in unstructured environments. Open-set object detection (OSOD) is a promising direction to handle the problem consisting of two subtasks: objects and background separation, and open-set object classification. In this paper, we present **Openset RCNN** to address the challenging OSOD. To disambiguate unknown objects and background in the first subtask, we propose to use classification-free region proposal network (CF-RPN) which estimates the objectness score of each region purely using cues from object’s location and shape preventing overfitting to the training categories. To identify unknown objects in the second subtask, we propose to represent them using the complementary region of known categories in a latent space which is accomplished by a prototype learning network (PLN). PLN performs instance-level contrastive learning to encode proposals to a latent space and builds a compact region centering with a prototype for each known category. Further, we note that the detection performance of unknown objects can not be unbiasedly evaluated on the situation that commonly used object detection datasets are not fully annotated. Thus, a new benchmark is introduced by reorganizing GraspNet-1billion, a robotic grasp pose detection dataset with complete annotation. Extensive experiments demonstrate the merits of our method. We finally show that our Openset RCNN can endow the robot with an open-set perception ability to support robotic rearrangement tasks in cluttered environments. More details can be found in <https://sites.google.com/view/openest-rcnn/>

## I. INTRODUCTION

When a robot executes manipulation tasks in unstructured environments, it will encounter unknown objects together with known objects. The task may fail if unknown objects are not being correctly perceived. Although significant achievements have been made in object detection [1]–[3], most object detectors assume that only a subset of training categories will appear in testing phase. Since object categories in real-world are infinite, close-set object detectors are not practical for the robot to work in the unstructured environments.

To endow the robot’s ability to detect both known and unknown objects, a potential solution is open-set object detection (OSOD), where the detector trained on *close-set* datasets is asked to detect all known objects and identify unknown objects in *open-set* conditions [4]. Apparently, OSOD is composed of two subtasks: 1) objects and background separation, 2) open-set object classification. An intuitive illustration showing the difference between close-set and open-set object detection for robotic manipulation is presented in Fig. 1.

Zhongxiang Zhou, Yifei Yang, Yue Wang and Rong Xiong are with the State Key Laboratory of Industrial Control Technology and Institute of Cyber-Systems and Control, Zhejiang University, Zhejiang, China. Yue Wang is the corresponding author [ywang24@zju.edu.cn](mailto:ywang24@zju.edu.cn)

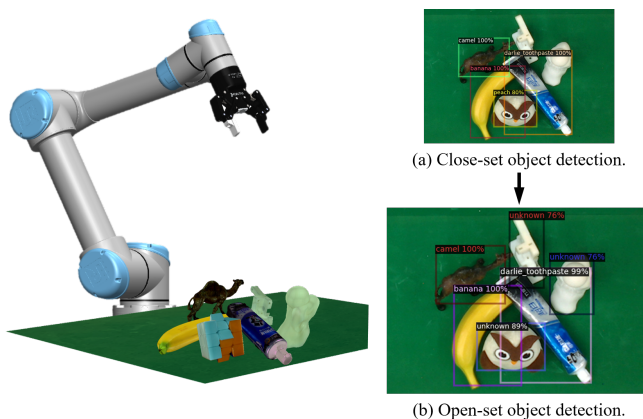


Fig. 1. (a) Close-set object detection assumes that object categories appearing in the testing phase are contained by training categories. When encountering unknown objects, a close-set object detector tends to simply ignore them or misclassify unknown objects to known categories. (b) Open-set object detection also trains a model on *close-set* datasets, but it is asked to detect all known objects and unknown objects in *open-set* conditions.

Lately, several works attempted to solve the challenging OSOD. Dhamija et al. [5] first formalized OSOD task and concluded that close-set object detectors suffer from performance degradation in the open-set conditions. Miller et al. [6], [7] studied the utility of Dropout Sampling [8] and Gaussian Mixture Models for estimating uncertainty which is used to identify open-set errors. Joseph et al. [9] proposed an energy-based unknown identifier by modeling the energy values of known and unknown categories. Han et al. [4] presented an unknown probability learner which is used to directly predict the known and unknown probabilities of proposals. However, prior works focus on the second subtask of OSOD improving the open-set classification ability. **And unknown objects are treated in the same way as one of the known classes which is characterized using a point or region in latent space.** We note that unknown objects may contain more than one category, representing all unknown objects using a single latent point or region is **inaccurate**.

As for how to separate objects and background, previous methods rely on **classification based** Region Proposal Network (RPN) [1]. Recently, Kim et al. [10] noticed that RPN tends to overfit to the training categories if using the binary classifier for close-set training. Because proposals for unknown objects would be regarded as negatives by the classification loss, impeding OSOD performance. Moreover, commonly used datasets such as PASCAL VOC [11] and COCO [12] do not exhaustively label all objects, **detections on unannotated objects will be regarded as false positives**

making the evaluation of unknown objects biased.

In this paper, we present Openset RCNN with classification-free RPN (CF-RPN) and prototype learning network (PLN) to address the challenging OSOD. CF-RPN learns object proposals using cues from object’s location and shape without classification to enhance generalization ability for unknown object proposals. PLN performs instance-level contrastive learning to encode proposals in a latent space and learning a discriminative representation called prototype for each known category. Benefiting from intra-class compactness and inter-class separation in the learnt latent space, known and unknown objects can be identified using distances between encoded proposals and prototypes. In this way, the complementary region of known categories in latent space can be used to represent unknown objects covering more unknown categories. Followed by a softmax classifier, known proposals are further classified into known categories.

To validate the effectiveness of our method, we first take VOC for close-set training and conduct open-set testing using both VOC and COCO which is the same as [4]. Differently, we do not adopt Average Precision of unknown as the evaluation metric since objects in VOC and COCO are not fully annotated. Furthermore, GraspNet-1billion [13], a robotic grasp pose detection dataset with complete annotation, is reorganized to form a new benchmark considering several open-set settings for fair comparison. Experimental results demonstrate that our method improves OSOD performance. Finally, we apply the proposed method to [five robotic rearrangement tasks](#) to manipulate known and unknown objects differently. Our contributions can be summarized as follows:

- A novel method, Openset RCNN, is proposed to [enhance generalization and identification ability for unknown objects with the help of CF-RPN and instance-level contrastive learning based PLN.](#)
- We introduce a new OSOD benchmark by reorganizing a fully annotated dataset called GraspNet-1billion [that can be used for an unbiased evaluation for OSOD and is more suitable for robot manipulation.](#)
- Extensive experiments demonstrate the merits of our method. And we show that our method can support robotic rearrangement tasks in cluttered environments.

## II. RELATED WORK

### A. Open Set Recognition

Scheirer et al. [14] first formalized OSR as an open risk minimization problem and developed an open-set classifier using linear SVMs. Their pioneering work inspired follow-up SVM-based approaches [15]–[17]. Recently, deep learning-based OSR methods have aroused extensive attention. Bendale et al. [18] introduced the first deep learning approach for OSR by replacing the SoftMax function with OpenMax function. Neal et al. [19] utilized GAN to synthesize unseen-class images and trained an open-set classifier with the generated images augmented training dataset. OpenGAN [20] found that it was more efficient to generate open-set features rather than realistic images, then an adversarially trained

discriminator was used to classify unknown examples. Other approaches include auto-encoder-based methods which use reconstruction errors as indicators of unknown identification [21], and prototype-based methods which identify unknowns by measuring the distances between image features and learned prototypes [22]. In addition, Vaze et al. [23] investigated that good close-set classifier benefits OSR. However, OSR can only recognize objects at the image level which limits its applications in robotic manipulation tasks.

### B. Open Set Object Detection

Dhamija et al. [5] first migrated the open-set setting to the object detection field. They noticed that objects from unknown classes were often incorrectly detected as known objects. In the context that uncertainty may indicate open-set errors, Miller et al. [6], [7] studied the utility of Dropout Sampling [8] and Gaussian Mixture Models to analyze the detector’s epistemic uncertainty and predictions with high uncertainty were regarded as unknown objects. Several works are proposed by introducing unknown labels during training. Joseph et al. [9] introduced an energy-based unknown identifier by modeling the energy values of known and unknown samples. However, annotations of unknown objects are needed by their methods [9], [24] breaking the setting of OSOD. Based on a transformer-based object detector, OW-DETR [25] adopted the magnitude of the attention feature map as the objectness scores of proposals and top-k selection was performed for obtaining pseudo-unknowns. The pseudo-labeled unknowns along with the ground-truth known objects are employed as foreground objects during training. UC-OWOD [26] also used the same strategy to select unknown samples from unannotated areas. Han et al. [4] presented an unknown probability learner augmenting the K-way classifier with the K+1-way classifier where K+1 denoted the unknown class. In order to reserve the probability for unknown classes during close-set training, they considered that the probability of unknown class should be the largest if the logit of ground-truth class is removed. In summary, previous OSOD methods treat unknown objects in the same way as one of the known classes which is characterized using a point or region in latent space. Since unknown objects may contain more than one category, this characterization is inaccurate. In contrast, our method represents unknown objects using the complementary region of known classes covering more unknown categories.

### C. Contrastive Learning

Self-supervised representation learning has recently achieved state of the art performance with the help of contrastive learning [27]–[29]. To effectively leverage label information, supervised contrastive learning [30] has been proposed and applied to other tasks, such as few-shot object detection [31], semantic segmentation [32], zero-shot learning [33] and long-tailed image classification [34]. Our method applies instance-level supervised contrastive learning to encode proposals in a latent space and build a compact region centering with a prototype for each known category.

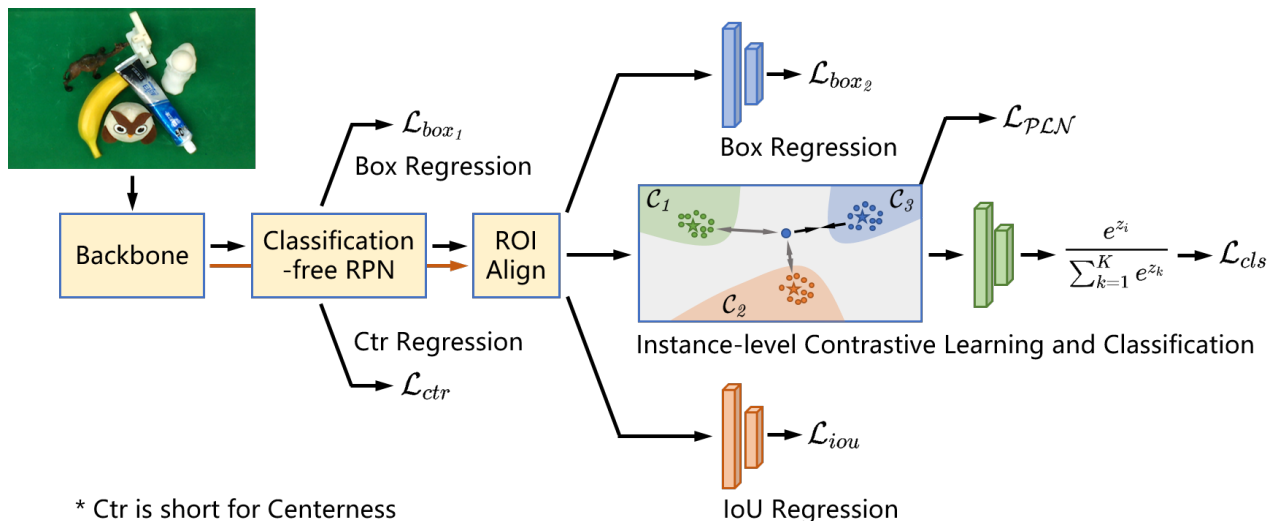


Fig. 2. Overview of the proposed open-set object detection method. Openset RCNN is endowed with classification-free RPN (CF-RPN) and prototype learning network (PLN) performing instance-level contrastive learning. CF-RPN learns to detect object proposals based on cues from object’s location and shape. PLN constructs a latent space which can be used to identify known and unknown objects using distances between encoded proposals and prototypes. Followed by a softmax classifier, known proposals are further classified into known categories.

### III. PROBLEM FORMALIZATION

We formally describe OSOD based on previous researches [4], [5], [9]. We denote two datasets  $D_{tr} = \{(x, y), x \in X_{tr}, y \in Y_{tr}\}$  and  $D_{te} = \{(x', y'), x' \in X_{te}, y' \in Y_{te}\}$ , where  $x$  and  $x'$  are input images with  $y$  and  $y'$  representing corresponding annotations including category label and coordinates of bounding box. An open-set object detector  $\mathcal{M}$  is trained using  $D_{tr}$  with image set  $X_{tr}$  and annotation set  $Y_{tr}$  containing  $K$  known categories  $C_K = \{c_1, \dots, c_k\}$ . Then  $\mathcal{M}$  is tested using  $D_{te}$  with image set  $X_{te}$  and annotation set  $Y_{te}$  containing  $K$  known categories as well as other unknown objects  $c_u \notin C_K$ . And  $\mathcal{M}$  is supposed to detect all known objects belonging to  $C_K$  and unknown objects  $c_u$  in  $D_{te}$ .

In general, OSOD is composed of two subtasks: 1) objects and background separation, 2) open-set objects classification. And two unique challenges are held by OSOD. Since  $D_{tr}$  may not be fully annotated, images in  $X_{tr}$  may contain annotated known objects and unannotated unknown objects. Accordingly, overfitting issue must be well addressed in OSOD. At the same time, complete annotation must be given in  $D_{te}$  in order to evaluate OSOD performance, especially on unknown objects.

### IV. METHODOLOGY

We present **Openset RCNN with classification-free RPN (CF-RPN) and instance-level contrastive learning based prototype learning network (PLN)**. The framework is shown in Fig. 2. ResNet-50 [35] with Feature Pyramid Network (FPN) [36] is used as the backbone network to extract feature maps of the input image. Classification-free RPN learns to detect object proposals based on cues from object’s location and shape. Then, instance-level contrastive learning is performed to encode proposals in a latent space and learn a discriminative representation called prototype for

each known category. After that, known and unknown objects can be identified using distances between encoded proposals and prototypes. Followed by a softmax classifier, known proposals are further classified into known categories.

#### A. Classification-free Region Proposal Network

To extract foreground objects in the image, **classification based RPN [1] is popularly used**. But classification based RPN often struggles to detect novel objects in open-set conditions because of overfitting to training categories. The overfitting issue is caused by two parts. On one hand, commonly used object detection datasets such as PASCAL VOC [11] and COCO [12] do not exhaustively label all objects, as shown in Fig. 3. On the other hand, binary classification loss is optimized with training categories as foreground and other unannotated objects as background.

Inspired by [10], we use CF-RPN in our open-set object detector to enhance generalization ability for unknown object proposals. Without supervision from category label, CF-RPN learns to detect objects using cues from object location and shape called localization quality. Specifically, binary classifier in standard RPN is replaced with centerness [37] regression. And *ltrb* bounding box regression is used to generate initial proposals instead of delta *xywh* regression according to the definition of centerness. Top-scoring proposals are taken to perform RoIAlign [38], then fed to bounding box refinement head and intersection-over-union (IoU) regression head. Both centerness score  $c$  and IoU score  $b$  are adopted to measure the quality of object proposal. **Following [10], objectness score is computed as a geometric mean of these two values  $s = \sqrt{c \cdot b}$ .**

During training, a proposal is considered as a positive sample if it has IoU greater than  $T_{pos}$  with the corresponding ground-truth box and a negative sample if IoU less than  $T_{neg}$ .

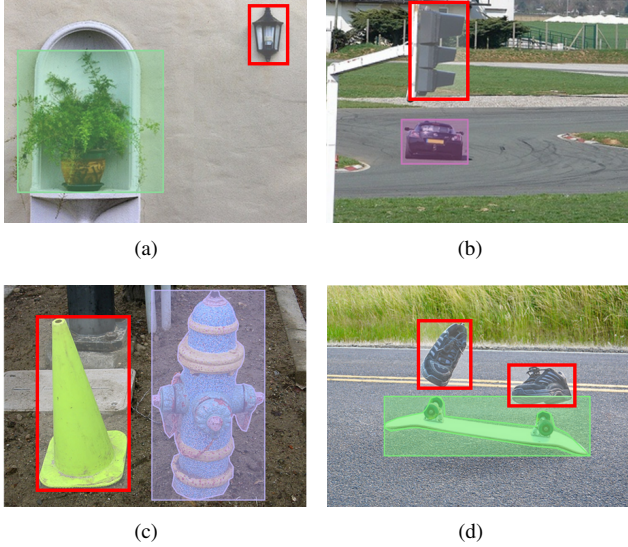


Fig. 3. Commonly used object detection datasets are not fully annotated, (a) PASCAL VOC trainval2007, (b) PASCAL VOC test2007, (c) COCO train2017 and (d) COCO val2017. Red boxes are objects without annotations and other colored boxes are annotated objects.

Then,  $N_s$  proposals are randomly sampled with positive fraction  $P_{pos}$  for loss computation. Our CF-RPN loss is formulated as:

$$\mathcal{L}_{CF-RPN} = \lambda_1 \mathcal{L}_{ctr} + \lambda_2 \mathcal{L}_{box_1} + \lambda_3 \mathcal{L}_{iou} + \lambda_4 \mathcal{L}_{box_2} \quad (1)$$

where  $\mathcal{L}_{ctr}$ ,  $\mathcal{L}_{box_1}$ ,  $\mathcal{L}_{iou}$  and  $\mathcal{L}_{box_2}$  are smooth L1 losses for centerness regression, *ltrb* bounding box regression, IoU regression and delta *xywh* bounding box regression. And  $\lambda_1$ ,  $\lambda_2$ ,  $\lambda_3$ , and  $\lambda_4$  are weighting coefficients. The first two losses are used for initial proposal generation and the last two losses are used for proposal refinement.

### B. Prototype Learning Network

To identify known and unknown objects from proposals generated by CF-RPN, we use PLN to construct a latent space and learn a discriminative representation called prototype for each known category. Then, known and unknown objects can be identified using distances between encoded proposals and prototypes.

Our PLN uses the proposal feature  $\mathbf{f}_i \in \mathbb{R}^{d_f}$  after RoIAlign as input. Typically,  $d_f = 1024$  which is the same as Faster RCNN [1]. Then, we use an encoder to map  $\mathbf{f}_i$  to a low-dimensional embedding vector  $\mathbf{z}_i \in \mathbb{R}^{d_z}$  ( $d_z = 256$  by default) in the latent space. In detail, the encoder is a single fully connected layer with nonlinearity. Subsequently, we measure distances between proposal embedding  $\mathbf{z}_i$  and learnable prototypes  $\mathbf{P} = \{\mathbf{P}_1, \dots, \mathbf{P}_K\}$  of known categories by computing the [cosine similarity](#). Different from [9], we use the weights of a fully connected layer as prototypes with less memory costs while they need to maintain a fixed length queue for each known category to store the embedding vectors and prototypes are computed by averaging all

vectors in the queue. Next, intra-class compactness and inter-class separation are encouraged by optimizing the following double-margin contrastive loss:

$$\mathcal{L}_{\mathcal{P}\mathcal{L}\mathcal{N}} = y_{ij} \max(D_{ij} - m_p, 0) + \max_j [(1 - y_{ij}) \max(m_n - D_{ij}, 0)] \quad (2)$$

where  $D_{ij} = \frac{\mathbf{z}_i \cdot \mathbf{P}_j}{\|\mathbf{z}_i\| \|\mathbf{P}_j\|}$  is the [cosine similarity](#) between proposal embedding  $\mathbf{z}_i$  and prototype  $\mathbf{P}_j \in \mathbf{P}$ ,  $y_{ij}$  is an indicating variable with value 1 if  $\mathbf{z}_i$  and  $\mathbf{P}_j$  are from the same category and 0 otherwise. As for  $m_p$  and  $m_n$ , they are thresholds for positive pairs from the same category and negative pairs from different categories. Contrastive loss  $\mathcal{L}_{\mathcal{P}\mathcal{L}\mathcal{N}} = 0$  under the condition that distances between proposal embeddings and prototype of the same category are less than  $m_p$  and distances between proposal embeddings and prototypes of different categories are larger than  $m_n$ . Note that we optimize the latent space using proposals having  $\text{IoU} > T_{iou}$  in a mini-batch where  $T_{iou}$  is an IoU threshold between proposals and ground-truth boxes to ensure the proposals contain relevant semantics.

Although the latent space can be used to measure the distances between a proposal embedding and each prototype, the category of this proposal can be determined by the prototype with minimum distance. We find that the close-set classification performance of the latent space is not as well as the traditional softmax classifier. So after identifying known and unknown objects using the latent space constructed by PLN, we apply a softmax classifier on all known objects to classify them into each known category. And the 256-dim proposal embedding  $\mathbf{z}_i$  is remapped to 1024-dim to restore the detail information benefiting classification. The loss function  $\mathcal{L}_{cls}$  used for optimization is a cross entropy loss which is the same as Faster RCNN [1].

### C. Overall Optimization and Inference

In total, the network is trained by the following multi-task loss:

$$\mathcal{L} = \alpha \mathcal{L}_{CF-RPN} + \beta \mathcal{L}_{\mathcal{P}\mathcal{L}\mathcal{N}} + \gamma \mathcal{L}_{cls} \quad (3)$$

which is a combination of  $\mathcal{L}_{CF-RPN}$ ,  $\mathcal{L}_{\mathcal{P}\mathcal{L}\mathcal{N}}$  and  $\mathcal{L}_{cls}$  with weighting coefficients  $\alpha$ ,  $\beta$  and  $\gamma$ . To train CF-RPN, we set  $N_s = 256$ ,  $T_{pos} = 0.3$ ,  $T_{neg} = 0.1$  and  $P_{pos} = 1.0$  for optimizing centerness regression loss  $L_{ctr}$ , set  $N_s = 256$ ,  $T_{pos} = 0.7$ ,  $T_{neg} = 0.3$  and  $P_{pos} = 0.5$  for optimizing *ltrb* bounding box regression loss  $L_{box_1}$ , and set  $N_s = 512$ ,  $T_{pos} = 0.5$ ,  $T_{neg} = 0.5$  and  $P_{pos} = 0.25$  for optimizing IoU regression loss and delta *xywh* regression loss. To train PLN, we set  $m_p = 0.05$ ,  $m_n = 0.95$  and  $T_{iou} = 0.5$ . We set  $\alpha = 1$ ,  $\beta = 0.5$ ,  $\gamma = 0.8$  and  $\lambda_{1,2,3,4} = 0.5$  in order to optimize network on OpenDet benchmark, and set  $\alpha = 1$ ,  $\beta = 2$ ,  $\gamma = 1$  and  $\lambda_{1,2,3,4} = \{1, 10, 1, 2\}$  for optimizing on GraspNet-1billion dataset. [Ablation studies on hyper-parameters are available in Appendix-C.](#)

During training, top 2000 centerness scoring proposals without non-maximum suppression (NMS) are taken for

proposal refinement and the subsequent process. During inference, top 1000 centerness scoring proposals are sent to NMS at 0.7, RoIAlign and proposal refinement. Then, objectness scores  $s$  are calculated for each proposal following a filter to remove proposals with  $s < 0.05$ . Next, proposals are encoded to the latent space to compute distances between each prototype and unknown objects are identified if the minimum distance among all prototypes is larger than a predefined threshold  $T_u = 0.17$ . Subsequently, known objects are sent to softmax classifier to classify them into each category. Note that after NMS for known and unknown objects separately, top 50 objectness scoring known and top 50 objectness scoring unknown objects are selected as the final detections.

## V. EXPERIMENTS

To validate the proposed method, we first report the open-set object detection performance on OpenDet benchmark [4]. As mentioned before, commonly used object detection datasets are not fully annotated and the detection performance of unknown objects can not be unbiasedly evaluated. We introduce a new benchmark by reorganizing a completely annotated dataset, GraspNet-1billion [13], and the open-set object detection performance is also reported.

### A. Metrics

To evaluate the open-set object detection performance, we use the **Wilderness Impact** (WI) [5] to measure the degree of unknown objects misclassified to known classes:

$$WI = \left( \frac{P_{\mathcal{K}}}{P_{\mathcal{K} \cup \mathcal{U}}} - 1 \right) \times 100 \quad (4)$$

where  $P_{\mathcal{K}}$  and  $P_{\mathcal{K} \cup \mathcal{U}}$  denote the **precision of known classes in close-set and open-set condition, respectively**. Following [9], we report WI under the recall level of 0.8. Besides, we also use **Absolute Open-Set Error** (AOSE) [6] to count the number of unknown objects that get wrongly classified as any of the known class. Both WI and AOSE implicitly measure how effective the model is in handling unknown objects. Furthermore, we report the **mean Average Precision** (mAP) of known classes ( $mAP_{\mathcal{K}}$ ) to measure the close-set object detection performance. Different from [4], we use **Recall** of unknown objects ( $R_{\mathcal{U}}$ ) indicating the detection ability of the unknown classes rather than Average Precision. Since **False Positive** of unknown objects can not be counted on the situation that objects in VOC and COCO are not fully annotated. Thus, WI, AOSE, and  $R_{\mathcal{U}}$  are open-set metrics, and  $mAP_{\mathcal{K}}$  is a close-set metric.

### B. Comparison Methods

We compare Openset RCNN with the following methods: Faster RCNN (FR-CNN) [1], Dropout Sampling (DS) [6], PROSER [39] and OpenDet [4]. We do not compare with ORE [9] because ORE relies on a validation set with annotations for the unknowns which violates the original definition of OSOD. We use the official code of OpenDet and retrain all models.

### C. Results on OpenDet Benchmark

OpenDet benchmark [4] is constructed based on PASCAL VOC [11] and MS COCO [12]. The VOC07 train and VOC12 trainval splits are taken for close-set training and 20 VOC classes are regarded as known categories. To create open-set conditions, 60 non-VOC classes in COCO are set to be unknown and two settings are defined: **VOC-COCO- $\{\mathbf{T}_1, \mathbf{T}_2\}$** . Open-set classes are gradually increased in setting  $\mathbf{T}_1$  and Wilderness Ratio (WR) [5] is gradually increased in setting  $\mathbf{T}_2$ . Meanwhile, the VOC test2007 split is used to evaluate the close-set detection performance. The quantitative results on OpenDet benchmark are shown in Tab. I and Tab. II. Note that  $mAP_{\mathcal{K}}$  is calculated using VOC 2012 method. The proposed Openset RCNN outperforms other methods with a healthy margin on VOC-COCO-T1 and achieves comparable results on VOC-COCO-T2 with OpenDet. Some qualitative results are illustrated in Fig. 4(a). [More discussions about the results are in Appendix-B.](#)

### D. Results on GraspNet OSOD Benchmark

We introduce a new benchmark by reorganizing GraspNet-1billion [13], a robotic grasp pose detection dataset with complete annotation. We take 28 out of 88 classes as known categories and 9728 images are used for close-set training. Following the same way of creating open-set conditions in [4], we also define two settings: **GraspNet-OSOD- $\{\mathbf{T}_1, \mathbf{T}_2\}$** . For setting  $\mathbf{T}_1$ , we gradually increase open-set classes to build three joint datasets GraspNet-Test- $\{1, 2, 3\}$  containing  $\{23808, 31744, 38912\}$  images of 28 known classes and  $\{12, 34, 60\}$  unknown classes. For setting  $\mathbf{T}_2$ , we gradually increase WR to construct three joint datasets GraspNet-Test- $\{4, 5, 6\}$  containing  $\{5120, 10240, 15360\}$  images with  $WR = \{1, 2, 3\}$ . The results on GraspNet OSOD benchmark are shown in Tab. III and Tab. IV. Note that  $mAP_{\mathcal{K}}$  is calculated using COCO method. The proposed Openset RCNN outperforms other methods remarkably on all metrics. Some qualitative results are illustrated in Fig. 4(b).

### E. Ablation Studies

We conduct ablation experiments on **GraspNet-Test-6** to analyze the effect of our main components. Our baseline is based on Faster R-CNN [1] consisting of a ResNet-50 backbone, standard Region Proposal Network and R-CNN in which box regressor is set to class-agnostic. As shown in Tab. V, the proposed two modules, CF-RPN and PLN, reduce AOSE substantially. Because unknown objects are modeled using the complementary region of known categories in latent space,  **$AP_{\mathcal{U}}$  of the PLN equipped baseline model (37.30) outperforms DS [6] and OpenDet [4] (27.27 and 36.55 in Tab. IV)**. And the combination of CF-RPN and PLN further improves the performance which verifies the effectiveness of the proposed components.

### F. Application in Robotic Rearrangement Tasks

We use the proposed method to demonstrate robotic object rearrangement in a cluttered environment using a UR5 collaborative robot with a Robotiq gripper and an external

TABLE I  
COMPARISONS WITH OTHER METHODS ON VOC AND VOC-COCO-T1.

Method	VOC	VOC-COCO-20				VOC-COCO-40				VOC-COCO-80			
	mAP <sub>K</sub> ↑	WI <sub>↓</sub>	AOSE <sub>↓</sub>	mAP <sub>K</sub> ↑	R <sub>U</sub> ↑	WI <sub>↓</sub>	AOSE <sub>↓</sub>	mAP <sub>K</sub> ↑	R <sub>U</sub> ↑	WI <sub>↓</sub>	AOSE <sub>↓</sub>	mAP <sub>K</sub> ↑	R <sub>U</sub> ↑
FR-CNN [1]	82.68	21.43	15058	58.22	0.00	25.92	23070	55.01	0.00	20.25	23216	55.44	0.00
PROSER [39]	81.84	21.18	13993	56.97	37.85	26.13	21676	53.86	25.39	20.55	22499	54.60	12.75
DS [6]	82.51	17.30	13031	58.39	19.67	20.93	19920	55.41	13.04	16.76	21749	56.11	5.38
OpenDet [4]	82.09	13.71	12080	58.08	36.52	16.56	18116	54.90	24.87	13.38	20790	55.88	12.79
Openset RCNN	<b>82.94</b>	<b>11.58</b>	<b>10839</b>	<b>59.19</b>	<b>50.22</b>	<b>14.48</b>	<b>16652</b>	<b>56.12</b>	<b>40.42</b>	<b>12.41</b>	<b>19631</b>	<b>57.01</b>	<b>28.66</b>

TABLE II  
COMPARISONS WITH OTHER METHODS ON VOC-COCO-T2.

Method	VOC-COCO-2500				VOC-COCO-5000				VOC-COCO-20000			
	WI <sub>↓</sub>	AOSE <sub>↓</sub>	mAP <sub>K</sub> ↑	R <sub>U</sub> ↑	WI <sub>↓</sub>	AOSE <sub>↓</sub>	mAP <sub>K</sub> ↑	R <sub>U</sub> ↑	WI <sub>↓</sub>	AOSE <sub>↓</sub>	mAP <sub>K</sub> ↑	R <sub>U</sub> ↑
FR-CNN [1]	8.93	5795	77.62	0.00	15.21	11711	74.59	0.00	32.93	47013	64.01	0.00
PROSER [39]	10.13	5452	76.66	28.56	17.67	11057	73.49	27.80	36.59	44403	62.37	28.45
DS [6]	8.23	4985	77.83	16.50	13.93	9755	74.83	16.28	31.28	39076	64.72	16.54
OpenDet [4]	6.51	4308	77.86	30.32	11.45	8600	75.36	28.75	25.14	34382	64.88	29.70
Openset RCNN	<b>6.66</b>	<b>3993</b>	<b>77.85</b>	<b>50.24</b>	<b>11.59</b>	<b>7705</b>	<b>74.90</b>	<b>49.67</b>	<b>24.87</b>	<b>30858</b>	<b>63.48</b>	<b>50.16</b>

TABLE III  
COMPARISONS WITH OTHER METHODS ON GRASPNET-OSOD-T1.

Method	GraspNet-Test-1				GraspNet-Test-2				GraspNet-Test-3			
	WI <sub>↓</sub>	AOSE <sub>↓</sub>	mAP <sub>K</sub> ↑	AP <sub>U</sub> ↑	WI <sub>↓</sub>	AOSE <sub>↓</sub>	mAP <sub>K</sub> ↑	AP <sub>U</sub> ↑	WI <sub>↓</sub>	AOSE <sub>↓</sub>	mAP <sub>K</sub> ↑	AP <sub>U</sub> ↑
FR-CNN [1]	0.09	124433	66.95	0.00	0.21	288090	62.57	0.00	0.25	403598	61.53	0.00
PROSER [39]	0.10	89567	68.27	33.70	0.25	212522	63.71	44.33	0.29	304243	62.75	44.85
DS [6]	0.12	89786	67.60	23.24	0.27	217794	63.06	26.73	0.31	310439	61.89	26.62
OpenDet [4]	0.11	91559	67.75	22.50	0.24	212260	63.66	33.30	0.29	306129	62.31	35.12
Openset RCNN	<b>0.05</b>	<b>19761</b>	<b>69.60</b>	<b>39.31</b>	<b>0.17</b>	<b>60051</b>	<b>66.34</b>	<b>44.75</b>	<b>0.20</b>	<b>85827</b>	<b>65.40</b>	<b>46.02</b>

TABLE IV  
COMPARISONS WITH OTHER METHODS ON GRASPNET-OSOD-T2.

Method	GraspNet-Test-4				GraspNet-Test-5				GraspNet-Test-6			
	WI <sub>↓</sub>	AOSE <sub>↓</sub>	mAP <sub>K</sub> ↑	AP <sub>U</sub> ↑	WI <sub>↓</sub>	AOSE <sub>↓</sub>	mAP <sub>K</sub> ↑	AP <sub>U</sub> ↑	WI <sub>↓</sub>	AOSE <sub>↓</sub>	mAP <sub>K</sub> ↑	AP <sub>U</sub> ↑
FR-CNN [1]	0.10	48804	68.19	0.00	0.24	156053	61.34	0.00	0.28	236779	59.35	0.00
PROSER [39]	0.09	34878	69.24	32.35	0.25	115422	62.15	47.03	0.30	177889	60.57	45.02
DS [6]	0.11	35080	68.72	23.95	0.29	118285	61.99	28.87	0.35	182647	59.94	27.27
OpenDet [4]	0.11	35560	69.16	22.11	0.28	115177	62.97	37.16	0.34	178976	60.44	36.55
Openset RCNN	<b>0.04</b>	<b>8277</b>	<b>71.47</b>	<b>38.30</b>	<b>0.21</b>	<b>32952</b>	<b>66.25</b>	<b>47.63</b>	<b>0.25</b>	<b>50942</b>	<b>64.92</b>	<b>46.91</b>

RGB-D camera. The task is to collect objects from a table and put known objects in bin A and unknown objects in bin B. Objects are detected using the proposed method and the point cloud of the scene is fed to GraspNet [13] to generate 6-DOF candidate grasps. The grasp that has the maximum score and locate within the detected bounding box is chosen to execute. Fig. 5 shows the open-set detection results at different stages of the task and also the execution of the robot grasps. Further, we compare the performance of PROSER [39], OpenDet [4] and the proposed Openset

RCNN in five robotic rearrangement tasks containing {3, 5, 7, 9, 11} objects respectively. Each task is conducted 5 times. The average task completion rate is reported in Fig. 6 and the proposed method outperforms the others. In detail, we investigate the number of objects wrongly detected and the results are shown in Fig. 7. More experimental results of each task can be found in Appendix-D.

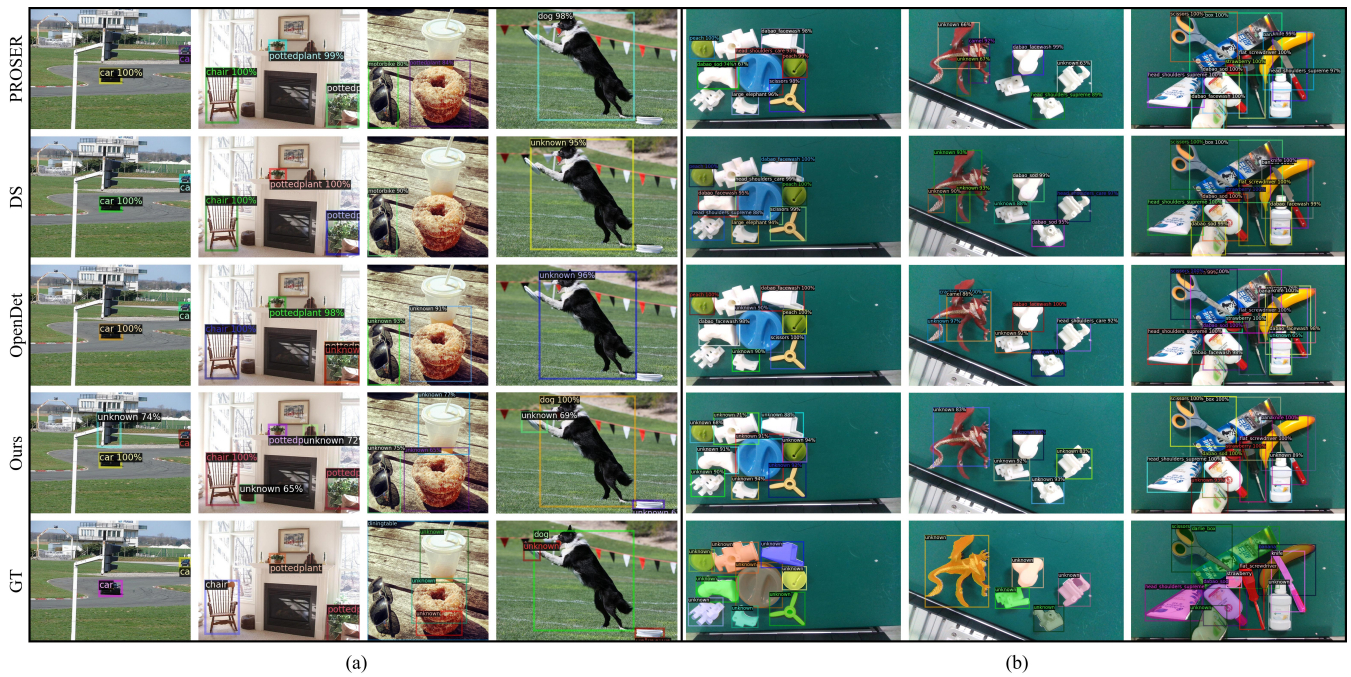


Fig. 4. Qualitative comparisons between Openset RCNN and other methods on (a) OpenDet benchmark [4] and (b) GraspNet OSOD benchmark.

TABLE V  
EFFECT OF DIFFERENT COMPONENTS ON GRASPNET-TEST-6.

CF-RPN	PLN	WI <sub>↓</sub>	AOSE <sub>↓</sub>	mAP <sub>K</sub> ↑	AP <sub>U</sub> ↑
		0.27	254027	61.15	0.00
✓		0.29	236594	61.24	0.00
	✓	0.39	69339	63.00	37.30
✓	✓	<b>0.25</b>	<b>50942</b>	<b>64.92</b>	<b>46.91</b>

## VI. CONCLUSIONS

In this work, we investigate the challenging open-set object detection for robotic manipulation and propose a novel method, Openset RCNN, with enhanced generalization ability for unknown object proposals as well as open-set classification. We also build an OSOD benchmark by reorganizing GraspNet-1billion dataset and conduct extensive experiments to demonstrate the effectiveness of our method. Finally, we show that our method can be applied to the robotic rearrangement task in cluttered environments supporting the robot to manipulate known and unknown objects differently. [More analysis and experiments can be accessed at Appendix.](#)

## REFERENCES

- [1] S. Ren, K. He, R. Girshick, and J. Sun, “Faster r-cnn: Towards real-time object detection with region proposal networks,” *Advances in neural information processing systems*, vol. 28, 2015.
- [2] J. Redmon, S. Divvala, R. Girshick, and A. Farhadi, “You only look once: Unified, real-time object detection,” in *Proceedings of the IEEE conference on computer vision and pattern recognition*, 2016, pp. 779–788.
- [3] N. Carion, F. Massa, G. Synnaeve, N. Usunier, A. Kirillov, and S. Zagoruyko, “End-to-end object detection with transformers,” in *European conference on computer vision*. Springer, 2020, pp. 213–229.

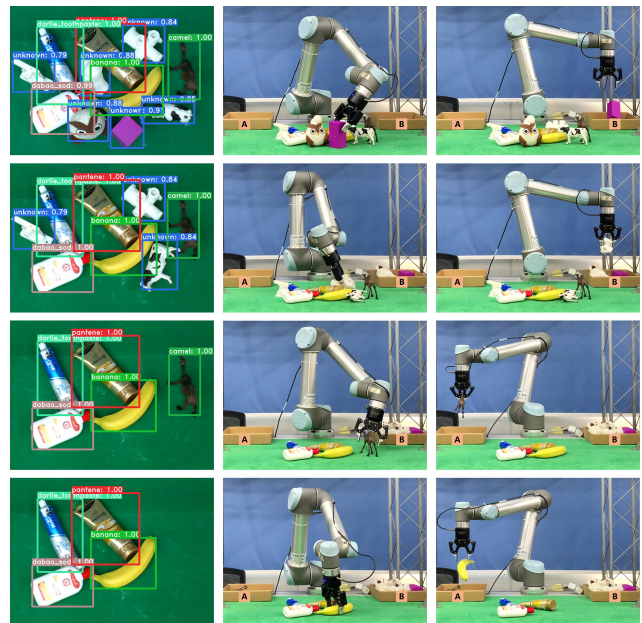


Fig. 5. Visualization of robotic rearrangement using the proposed detection method and 6-DOF GraspNet [13].

- [4] J. Han, Y. Ren, J. Ding, X. Pan, K. Yan, and G.-S. Xia, “Expanding low-density latent regions for open-set object detection,” in *Proceedings of the IEEE/CVF Conference on Computer Vision and Pattern Recognition (CVPR)*, 2022.
- [5] A. Dhamija, M. Gunther, J. Ventura, and T. Boulton, “The overlooked elephant of object detection: Open set,” in *Proceedings of the IEEE/CVF Winter Conference on Applications of Computer Vision*, 2020, pp. 1021–1030.
- [6] D. Miller, L. Nicholson, F. Dayoub, and N. Sünderhauf, “Dropout sampling for robust object detection in open-set conditions,” in *2018 IEEE International Conference on Robotics and Automation (ICRA)*. IEEE, 2018, pp. 3243–3249.
- [7] D. Miller, N. Sünderhauf, M. Milford, and F. Dayoub, “Uncertainty for

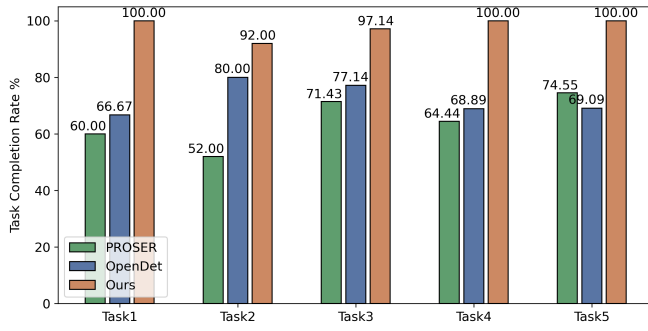


Fig. 6. The average task completion rate of 5 robotic rearrangement tasks using PROSER [39], OpenDet [4] and the proposed Openset RCNN.

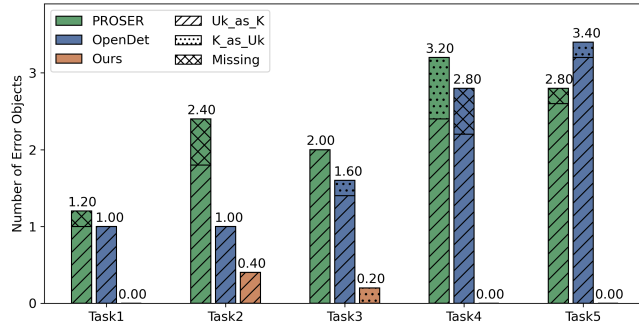


Fig. 7. The number of wrongly detected objects in 5 robotic rearrangement tasks using PROSER [39], OpenDet [4] and the proposed Openset RCNN. “UK.as.K” means unknown objects are detected as one of the known categories. “K.as.Uk” means known objects are detected as unknown and “Missing” means objects are detected as background.

identifying open-set errors in visual object detection,” *IEEE Robotics and Automation Letters*, vol. 7, no. 1, pp. 215–222, 2021.

- [8] Y. Gal and Z. Ghahramani, “Dropout as a bayesian approximation: Representing model uncertainty in deep learning,” in *international conference on machine learning*. PMLR, 2016, pp. 1050–1059.
- [9] K. Joseph, S. Khan, F. S. Khan, and V. N. Balasubramanian, “Towards open world object detection,” in *Proceedings of the IEEE/CVF Conference on Computer Vision and Pattern Recognition*, 2021, pp. 5830–5840.
- [10] D. Kim, T.-Y. Lin, A. Angelova, I. S. Kweon, and W. Kuo, “Learning open-world object proposals without learning to classify,” *IEEE Robotics and Automation Letters*, vol. 7, no. 2, pp. 5453–5460, 2022.
- [11] M. Everingham, L. Van Gool, C. K. Williams, J. Winn, and A. Zisserman, “The pascal visual object classes (voc) challenge,” *International journal of computer vision*, vol. 88, no. 2, pp. 303–338, 2010.
- [12] T.-Y. Lin, M. Maire, S. Belongie, J. Hays, P. Perona, D. Ramanan, P. Dollár, and C. L. Zitnick, “Microsoft coco: Common objects in context,” in *European conference on computer vision*. Springer, 2014, pp. 740–755.
- [13] H.-S. Fang, C. Wang, M. Gou, and C. Lu, “Graspnet-1billion: A large-scale benchmark for general object grasping,” in *Proceedings of the IEEE/CVF Conference on Computer Vision and Pattern Recognition*, 2020, pp. 11 444–11 453.
- [14] W. J. Scheirer, A. de Rezende Rocha, A. Sapkota, and T. E. Boulton, “Toward open set recognition,” *IEEE transactions on pattern analysis and machine intelligence*, vol. 35, no. 7, pp. 1757–1772, 2012.
- [15] W. J. Scheirer, L. P. Jain, and T. E. Boulton, “Probability models for open set recognition,” *IEEE transactions on pattern analysis and machine intelligence*, vol. 36, no. 11, pp. 2317–2324, 2014.
- [16] L. P. Jain, W. J. Scheirer, and T. E. Boulton, “Multi-class open set recognition using probability of inclusion,” in *European Conference on Computer Vision*. Springer, 2014, pp. 393–409.
- [17] A. Bendale and T. Boulton, “Towards open world recognition,” in *Proceedings of the IEEE conference on computer vision and pattern recognition*, 2015, pp. 1893–1902.
- [18] A. Bendale and T. E. Boulton, “Towards open set deep networks,” in *Proceedings of the IEEE conference on computer vision and pattern recognition*, 2016, pp. 1563–1572.
- [19] L. Neal, M. Olson, X. Fern, W.-K. Wong, and F. Li, “Open set learning with counterfactual images,” in *Proceedings of the European Conference on Computer Vision (ECCV)*, 2018, pp. 613–628.
- [20] S. Kong and D. Ramanan, “Opengan: Open-set recognition via open data generation,” in *Proceedings of the IEEE/CVF International Conference on Computer Vision*, 2021, pp. 813–822.
- [21] X. Sun, Z. Yang, C. Zhang, K.-V. Ling, and G. Peng, “Conditional gaussian distribution learning for open set recognition,” in *Proceedings of the IEEE/CVF Conference on Computer Vision and Pattern Recognition*, 2020, pp. 13 480–13 489.
- [22] H.-M. Yang, X.-Y. Zhang, F. Yin, Q. Yang, and C.-L. Liu, “Convolutional prototype network for open set recognition,” *IEEE Transactions on Pattern Analysis and Machine Intelligence*, 2020.
- [23] S. Vaze, K. Han, A. Vedaldi, and A. Zisserman, “Open-set recognition: a good closed-set classifier is all you need?” in *International Conference on Learning Representations*, 2022.
- [24] D. K. Singh, S. N. Rai, K. Joseph, R. Saluja, V. N. Balasubramanian, C. Arora, A. Subramanian, and C. Jawahar, “Order: Open world object detection on road scenes.”
- [25] A. Gupta, S. Narayan, K. Joseph, S. Khan, F. S. Khan, and M. Shah, “Ow-detr: Open-world detection transformer,” in *Proceedings of the IEEE/CVF Conference on Computer Vision and Pattern Recognition*, 2022, pp. 9235–9244.
- [26] Z. Wu, Y. Lu, X. Chen, Z. Wu, L. Kang, and J. Yu, “Uc-owod: Unknown-classified open world object detection,” *arXiv preprint arXiv:2207.11455*, 2022.
- [27] K. He, H. Fan, Y. Wu, S. Xie, and R. Girshick, “Momentum contrast for unsupervised visual representation learning,” in *Proceedings of the IEEE/CVF conference on computer vision and pattern recognition*, 2020, pp. 9729–9738.
- [28] Y. Tian, C. Sun, B. Poole, D. Krishnan, C. Schmid, and P. Isola, “What makes for good views for contrastive learning?” *Advances in Neural Information Processing Systems*, vol. 33, pp. 6827–6839, 2020.
- [29] R. Qian, T. Meng, B. Gong, M.-H. Yang, H. Wang, S. Belongie, and Y. Cui, “Spatiotemporal contrastive video representation learning,” in *Proceedings of the IEEE/CVF Conference on Computer Vision and Pattern Recognition*, 2021, pp. 6964–6974.
- [30] P. Khosla, P. Teterwak, C. Wang, A. Sarna, Y. Tian, P. Isola, A. Maschinot, C. Liu, and D. Krishnan, “Supervised contrastive learning,” *Advances in Neural Information Processing Systems*, vol. 33, pp. 18 661–18 673, 2020.
- [31] B. Sun, B. Li, S. Cai, Y. Yuan, and C. Zhang, “Fscf: Few-shot object detection via contrastive proposal encoding,” in *Proceedings of the IEEE/CVF Conference on Computer Vision and Pattern Recognition*, 2021, pp. 7352–7362.
- [32] X. Zhao, R. Vemulapalli, P. A. Mansfield, B. Gong, B. Green, L. Shapira, and Y. Wu, “Contrastive learning for label efficient semantic segmentation,” in *Proceedings of the IEEE/CVF International Conference on Computer Vision*, 2021, pp. 10 623–10 633.
- [33] Z. Han, Z. Fu, S. Chen, and J. Yang, “Contrastive embedding for generalized zero-shot learning,” in *Proceedings of the IEEE/CVF Conference on Computer Vision and Pattern Recognition*, 2021, pp. 2371–2381.
- [34] P. Wang, K. Han, X.-S. Wei, L. Zhang, and L. Wang, “Contrastive learning based hybrid networks for long-tailed image classification,” in *Proceedings of the IEEE/CVF Conference on Computer Vision and Pattern Recognition*, 2021, pp. 943–952.
- [35] K. He, X. Zhang, S. Ren, and J. Sun, “Deep residual learning for image recognition,” in *Proceedings of the IEEE conference on computer vision and pattern recognition*, 2016, pp. 770–778.
- [36] T.-Y. Lin, P. Dollár, R. Girshick, K. He, B. Hariharan, and S. Belongie, “Feature pyramid networks for object detection,” in *Proceedings of the IEEE conference on computer vision and pattern recognition*, 2017, pp. 2117–2125.
- [37] Z. Tian, C. Shen, H. Chen, and T. He, “Fcos: Fully convolutional one-stage object detection,” in *Proceedings of the IEEE/CVF international conference on computer vision*, 2019, pp. 9627–9636.
- [38] K. He, G. Gkioxari, P. Dollár, and R. Girshick, “Mask r-cnn,” in *Proceedings of the IEEE international conference on computer vision*, 2017, pp. 2961–2969.
- [39] D.-W. Zhou, H.-J. Ye, and D.-C. Zhan, “Learning placeholders for open-set recognition,” in *Proceedings of the IEEE/CVF Conference on Computer Vision and Pattern Recognition*, 2021, pp. 4401–4410.



## APPENDIX

### A. Comparisons with OW-DETR

Recently, OW-DETR [25] was proposed trying to handle open-world object detection using the transformer architecture. It adopted the magnitude of the attention feature map as the objectness scores of proposals and top-k selection was performed on the proposals having high objectness scores yet not overlapping with the ground-truth known instances for obtaining pseudo-unknowns. The pseudo-labeled unknowns along with the ground-truth known objects are employed as foreground objects during training.

We make evaluations using the protocol proposed by ORE [9] which is the same as OW-DETR. The protocol was designed for open-world object detection including four tasks to evaluate the performance of open-set object detection as well as incremental learning. Since incremental learning is not within the scope of our work, we only evaluate the proposed method on task 1 and make comparisons with OW-DETR. Specifically and following OW-DETR, the training dataset of task 1 contains 16551 images of 20 VOC classes and the testing dataset contains 10246 images of 20 VOC classes and 60 COCO classes for open-set evaluation.

The results are reported in Tab. VI showing the superiority of our Openset RCNN.

TABLE VI  
COMPARISON BETWEEN OPENSET RCNN AND OW-DETR ON  
OWOD-TASK-1.

Method	OWOD-Task-1			
	WI $\downarrow$	AOSE $\downarrow$	mAP $\mathcal{K}\uparrow$	R $\mathcal{U}\uparrow$
OW-DETR	5.71	10240	59.21	7.51
Openset RCNN	<b>4.67</b>	<b>5403</b>	<b>59.34</b>	<b>20.42</b>

### B. Analysis on OpenDet Benchmark

The comparison results on OpenDet benchmark [4] are reported in Tab. I and Tab. II in the main manuscript. Although the proposed Openset RCNN achieves the best results on VOC-COCO-T1, the performance on VOC-COCO-T2 need a further discussion. From Tab. II in the main manuscript, we can see that the AOSE and  $R_{\mathcal{U}}$  are better than existing methods and WI is considerably the same. However, mAP $\mathcal{K}$  underperforms OpenDet [4] especially in VOC-COCO-20000 which attracts our attention.

We compare the average precision of each known class between the proposed method and OpenDet [4] in Fig. 8. We can see that average precision of most classes is at the same level except that of diningtable. The diningtable’s average precision of OpenDet [4] is 57.78 while that of the proposed Openset RCNN is 11.00. From the construction of OpenDet benchmark [4], we notice that VOC-COCO-20000 contains 4952 close-set images from PASCAL VOC [11] and 20000 open-set images from COCO [12]. We then analyze the distribution of diningtable instances and report in Tab. VII. We can see that all annotations of diningtable are

contained by close-set images. A straightforward thinking would be comparing the detection performance only using 4952 close-set images and check if the bad results are caused by open-set images. These results are plotted in Fig. 9 and the average precision of diningtable in 4952 close-set images are 76.64(OpenDet) and 72.19(Openset RCNN). The gap is not that big. Thus, we affirm that the bad results of diningtable are actually caused by open-set images. Next, we investigate the number of detections classified as diningtable in 20000 open-set images. The results in Tab. VIII show that the proposed method detect more instances in 20000 open-set images which will be regarded as false positives since there are zero ground-truth annotations. After that, we visualize the detected diningtable instances of the proposed method. Some of the detections with confidence larger than 0.9 and not detected by OpenDet [4] are displayed in Fig. 10. By comparing with ground-truth diningtable instances used in training (see Fig. 11), we note that quite a lot of detections are indeed instances of diningtable but not annotated.

Based on the above analysis, we conclude that the underperforming mAP $\mathcal{K}$  in VOC-COCO-20000 is mainly caused by the abnormal detection results of diningtable class. By looking into the average precision of diningtable in 4952 close-set images and 20000 open-set images contained by VOC-COCO-20000. We verify that the detection performance of diningtable in 4952 close-set images is comparable(76.64 of OpenDet v.s. 72.19 of Openset RCNN) and the big gap between our Openset RCNN and OpenDet is actually caused by open-set images. Via checking the detections in 20000 open-set images, we find that many of them are actually instances of diningtable but not annotated. This is maybe caused by the annotation bias between PASCAL VOC [11] and COCO [12]. As stated in INTRODUCTION of the main manuscript, “Moreover, commonly used datasets such as PASCAL VOC and COCO do not exhaustively label all objects, detections on unannotated objects will be regarded as false positives making the evaluation of unknown objects biased.”, we think that the results on the proposed GraspNet OSOD benchmark are more fair-minded and informative.

### C. Ablation on Hyper-parameters

We conduct more ablation experiments on GraspNet-Test-6 to analyze the design choices of hyper-parameters.

**Classification-free region proposal network(CF-RPN).** We first study the selection of CF-RPN related parameters. In total, CF-RPN related parameters include IoU thresholds  $T_{pos}$  and  $T_{neg}$  for sampling positive and negative proposals, the number of proposals  $N_s$  and the fraction of positive samples  $P_{pos}$  used for loss computation. Following Faster RCNN [1], we keep  $N_s = 256$  for initial proposal generation and  $N_s = 512$ ,  $T_{pos} = 0.5$ ,  $T_{neg} = 0.5$  and  $P_{pos} = 0.25$  for bounding box refinement. Then, we investigate different choices of other parameters relating to initial proposal generation including IoU thresholds  $T_{pos}$  and  $T_{neg}$  as well as the fraction of positive samples  $P_{pos}$  in Tab. IX and Tab. X.

**Prototype learning network(PLN).** We further study the design choices of PLN related parameters. Specifically, PLN

related parameters contain feature dimension  $d_z$  in the latent space, distance thresholds  $m_p$  and  $m_n$  for positive pairs from the same category and negative pairs from different categories, IoU threshold  $T_{iou}$  to select proposals optimizing the latent space and the threshold  $T_u$  for known objects and unknown objects identification. Contrastive loss  $\mathcal{L}_{\mathcal{P}\mathcal{L}\mathcal{N}} = 0$  under the condition that distances between proposal embeddings and prototype of the same category are less than  $m_p$  and distances between proposal embeddings and prototypes of different categories are larger than  $m_n$ . The ablation results are reported in Tab. XI. The final parameters are chosen with this rule, improving detection performance of unknown objects should not sacrifice accuracy of close-set detection, in mind.

**Weighting coefficients of different losses.** We next study the weighting coefficients of different losses. The proposed Openset RCNN uses six loss functions with corresponding coefficients which is formulated as Equ. 3. The ablation results are reported in Tab. XIII. From the results, we can see that PLN plays a key role for reducing AOSE.

#### D. More Results on Robotic Rearrangement Tasks

We conduct five robotic object rearrangement tasks and each task contains  $\{3, 5, 7, 9, 11\}$  objects. The number of known and unknown objects in each task is reported in Tab. XII. Then, we randomly set five cases for each task and the detailed setting of robotic object rearrangement tasks are displayed in Fig. 12. The task is to collect objects from a table and put known objects in the left paper box and unknown objects in the right paper box. During testing, the confidence threshold of known categories is set to 0.85 and the confidence threshold of unknown category is set to 0.8. These two thresholds are set empirically and not optimized intentionally for our method. The results of task completion rate are shown in Fig. 13. In addition, we investigate the number of objects wrongly detected in each task and display the results in Fig.14. From the results, the proposed Openset RCNN outperforms the compared methods with a healthy margin. The number of misclassified objects or missed objects is much less than other methods.

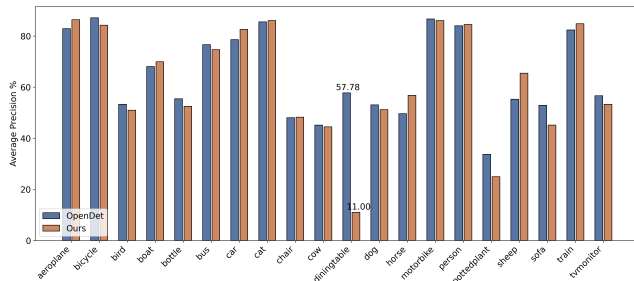


Fig. 8. Average precision of each known class in VOC-COCO-20000. We can see that average precision of most classes is at the same level except that of diningtable(57.78 v.s. 11.00).

TABLE VII

DISTRIBUTION OF DININGTABLE INSTANCE IN VOC-COCO-20000.

Dataset	VOC-COCO-20000	
Total number of diningtable	299	
Dataset composition	4952 close-set images	20000 open-set images
Number of diningtable	299	0

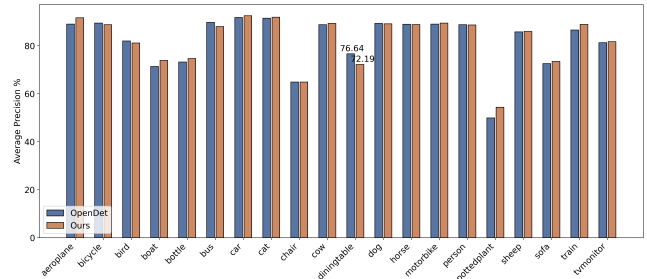


Fig. 9. Average precision of each known class in 4952 close-set images contained by VOC-COCO-20000. The average precision of diningtable in 4952 close-set images are 76.64(OpenDet) and 72.19(Openset RCNN).

TABLE VIII

THE NUMBER OF DETECTIONS CLASSIFIED AS DINNINGTABLE IN 20000 OPEN-SET IMAGES.

Method	Openset RCNN	OpenDet
Number of detections in 4952 close-set images	1473	1680
Number of detections in 20000 open-set images	6688	4999

TABLE IX

ABLATION STUDY OF CENTERNESS REGRESSION RELATED PARAMETERS ON GRASPNET-TEST-6. THE FINAL PARAMETERS APPLIED IN MAIN EXPERIMENTS ARE HIGHLIGHTED USING BOLD.

$N_s$	256	<b>256</b>	256	256	256	256
$T_{pos}$	0.3	<b>0.3</b>	0.1	0.5	0.5	0.7
$T_{neg}$	0.1	<b>0.1</b>	0.1	0.1	0.3	0.3
$P_{pos}$	0.7	<b>1.0</b>	1.0	1.0	0.5	1.0
$WI_{\downarrow}$	0.26	<b>0.25</b>	0.29	0.28	0.27	0.27
$AOSE_{\downarrow}$	64534	<b>50942</b>	57928	71614	62726	65998
$mAP_{\mathcal{K}\uparrow}$	63.35	<b>64.92</b>	63.95	64.34	62.91	64.57
$AP_{\mathcal{U}\uparrow}$	48.17	<b>46.91</b>	47.95	51.04	49.35	48.93

TABLE X

ABLATION STUDY OF  $ltrb$  BOUNDING BOX REGRESSION RELATED PARAMETERS ON GRASPNET-TEST-6. THE FINAL PARAMETERS APPLIED IN MAIN EXPERIMENTS ARE HIGHLIGHTED USING BOLD.

$N_s$	256	<b>256</b>	256	256	256	256
$T_{pos}$	0.7	<b>0.7</b>	0.7	0.5	0.9	0.7
$T_{neg}$	0.3	<b>0.3</b>	0.3	0.3	0.3	0.1
$P_{pos}$	0.3	<b>0.5</b>	0.7	0.5	0.5	0.5
$WI_{\downarrow}$	0.25	<b>0.25</b>	0.24	0.25	0.29	0.28
$AOSE_{\downarrow}$	54968	<b>50942</b>	54371	54456	56760	52002
$mAP_{\mathcal{K}\uparrow}$	63.06	<b>64.92</b>	63.84	64.08	63.30	63.57
$AP_{\mathcal{U}\uparrow}$	46.71	<b>46.91</b>	48.22	45.56	46.64	46.77



Fig. 10. The detected dinningtable instances with confidence larger than 0.9 by the proposed Openset RCNN and not detected by OpenDet [4]. These images are all from COCO [12].



Fig. 11. The ground-truth dinningtable instances used in training. These images are all from PASCAL VOC [11].

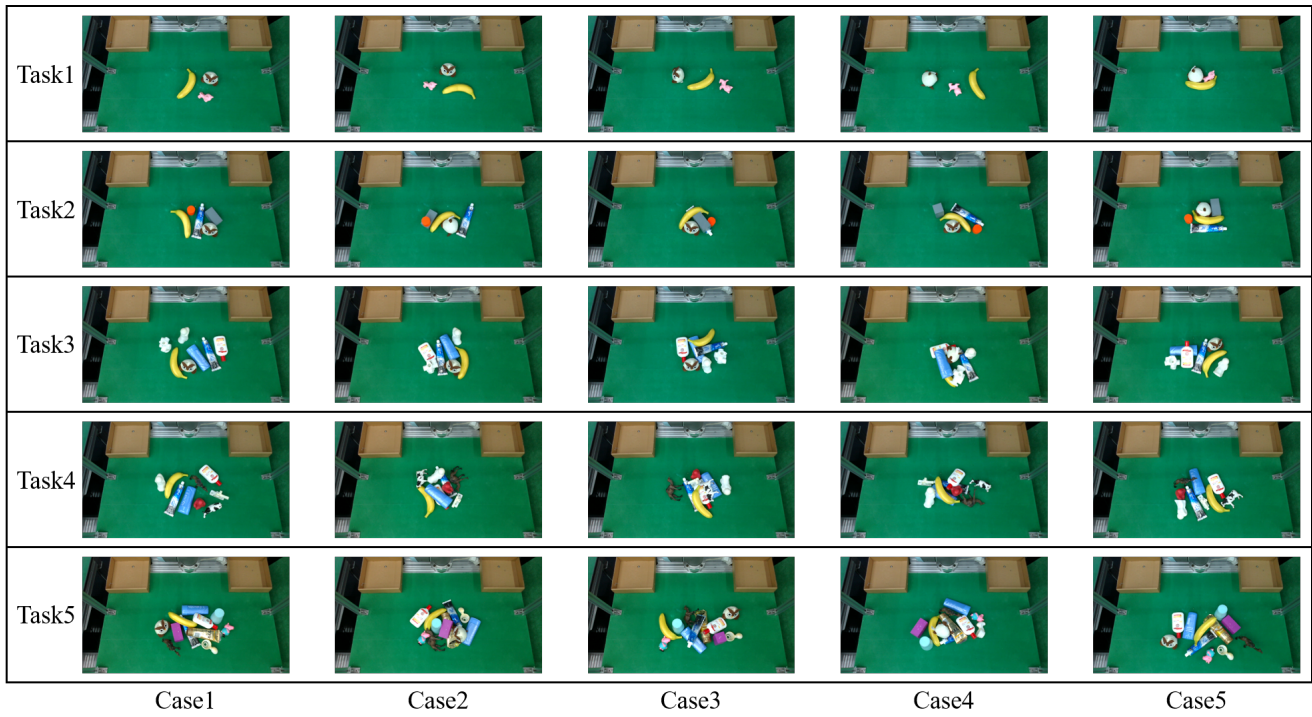


Fig. 12. The detailed setting of five robotic object rearrangement tasks.

TABLE XI

ABLATION STUDY OF PROTOTYPE LEARNING NETWORK RELATED PARAMETERS ON GRASPNET-TEST-6. THE FINAL PARAMETERS APPLIED IN MAIN EXPERIMENTS ARE HIGHLIGHTED USING BOLD.

$d_z$	256	<b>256</b>	256	256	128	256	256	256
$m_p$	0.05	<b>0.05</b>	0.05	0.1	0.05	0.05	0.05	0.05
$m_n$	0.95	<b>0.95</b>	0.95	0.9	0.95	0.95	0.95	0.95
$T_{iou}$	0.3	<b>0.5</b>	0.7	0.5	0.5	0.5	0.5	0.5
$T_u$	0.17	<b>0.17</b>	0.17	0.17	0.17	0.10	0.20	0.30
$WI_{\downarrow}$	0.26	<b>0.25</b>	0.31	0.23	0.27	0.24	0.25	0.28
$AOSE_{\downarrow}$	51126	<b>50942</b>	95419	34166	49745	21295	76136	212428
$mAP_{\mathcal{K}\uparrow}$	64.69	<b>64.92</b>	63.77	63.83	63.76	62.39	65.57	66.07
$AP_{\mathcal{U}\uparrow}$	47.69	<b>46.91</b>	45.66	50.95	47.50	54.99	42.62	19.91

TABLE XII

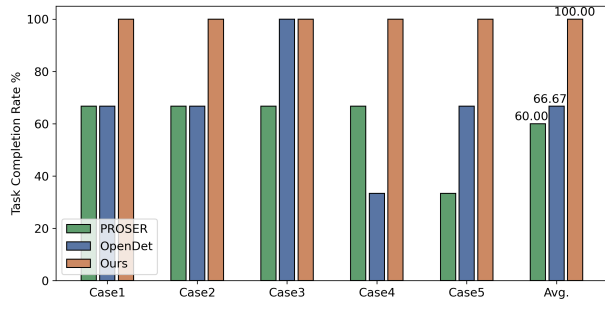
THE NUMBER OF KNOWN AND UNKNOWN OBJECTS IN EACH TASK.

	Total Number of Objects	Number of Known Objects	Number of Unknown Objects	Name of Known Objects
Task1	3	1	2	banana
Task2	5	2	3	banana, darlie_toothpaste
Task3	7	3	4	banana,dabao_sod darlie_toothpaste
Task4	9	4	5	banana,dabao_sod, darlie_toothpaste,camel
Task5	11	5	6	banana,darlie_toothpaste, dabao_sod,camel,pantene

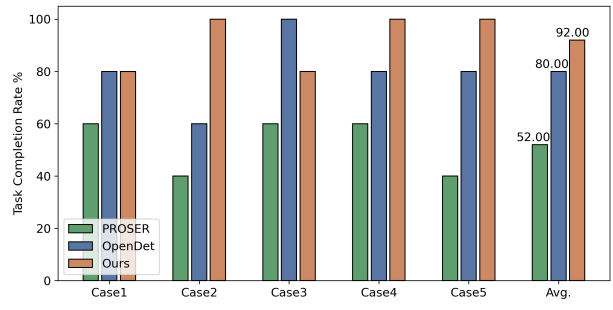
TABLE XIII

ABLATION STUDY OF WEIGHTING COEFFICIENTS OF DIFFERENT LOSSES ON GRASPNET-TEST-6. THE FINAL PARAMETERS APPLIED IN MAIN EXPERIMENTS ARE HIGHLIGHTED USING BOLD.

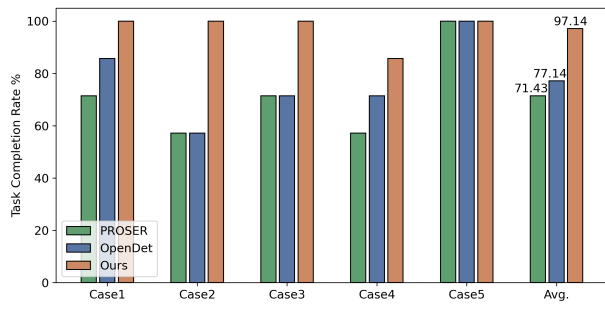
$\lambda_1$	1	1	1	1	1	<b>1</b>	5	5
$\lambda_2$	1	1	1	1	5	<b>10</b>	10	10
$\lambda_3$	1	1	1	1	1	<b>1</b>	10	10
$\lambda_4$	1	1	2	2	2	<b>2</b>	1	2
$\beta$	1	2	1	2	2	<b>2</b>	1	2
$\gamma$	1	1	1	1	1	<b>1</b>	1	1
$WI_{\downarrow}$	0.29	0.23	0.24	0.22	0.25	<b>0.25</b>	0.28	0.28
$AOSE_{\downarrow}$	113656	51103	143413	57029	51868	<b>50942</b>	121294	51557
$mAP_{\mathcal{K}\uparrow}$	63.56	62.68	65.11	64.44	63.91	<b>64.92</b>	63.88	64.47
$AP_{\mathcal{U}\uparrow}$	37.84	45.41	37.70	47.69	48.09	<b>46.91</b>	35.98	45.57



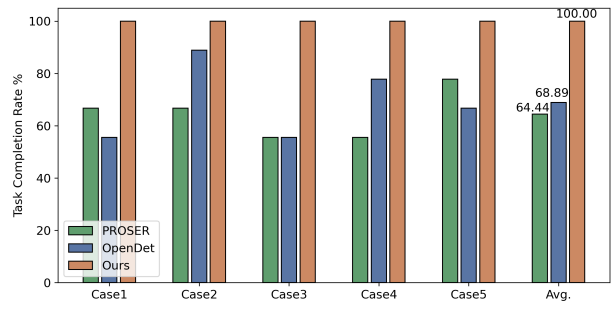
(a)



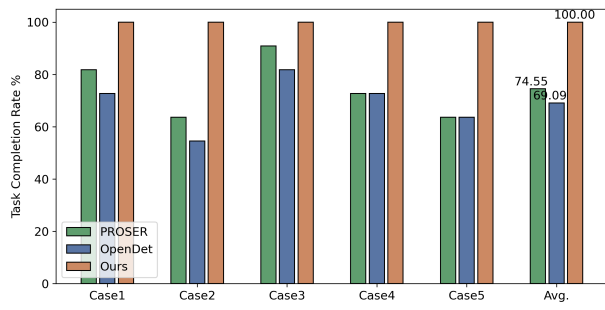
(b)



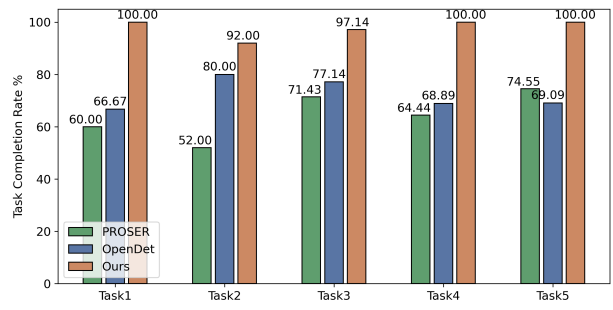
(c)



(d)



(e)



(f)

Fig. 13. Comparison of task completion rate. (a) Task completion rate in Task1, (b) Task completion rate in Task2, (c) Task completion rate in Task3, (d) Task completion rate in Task4, (e) Task completion rate in Task5, (f) Average of task completion rate in 5 tasks.

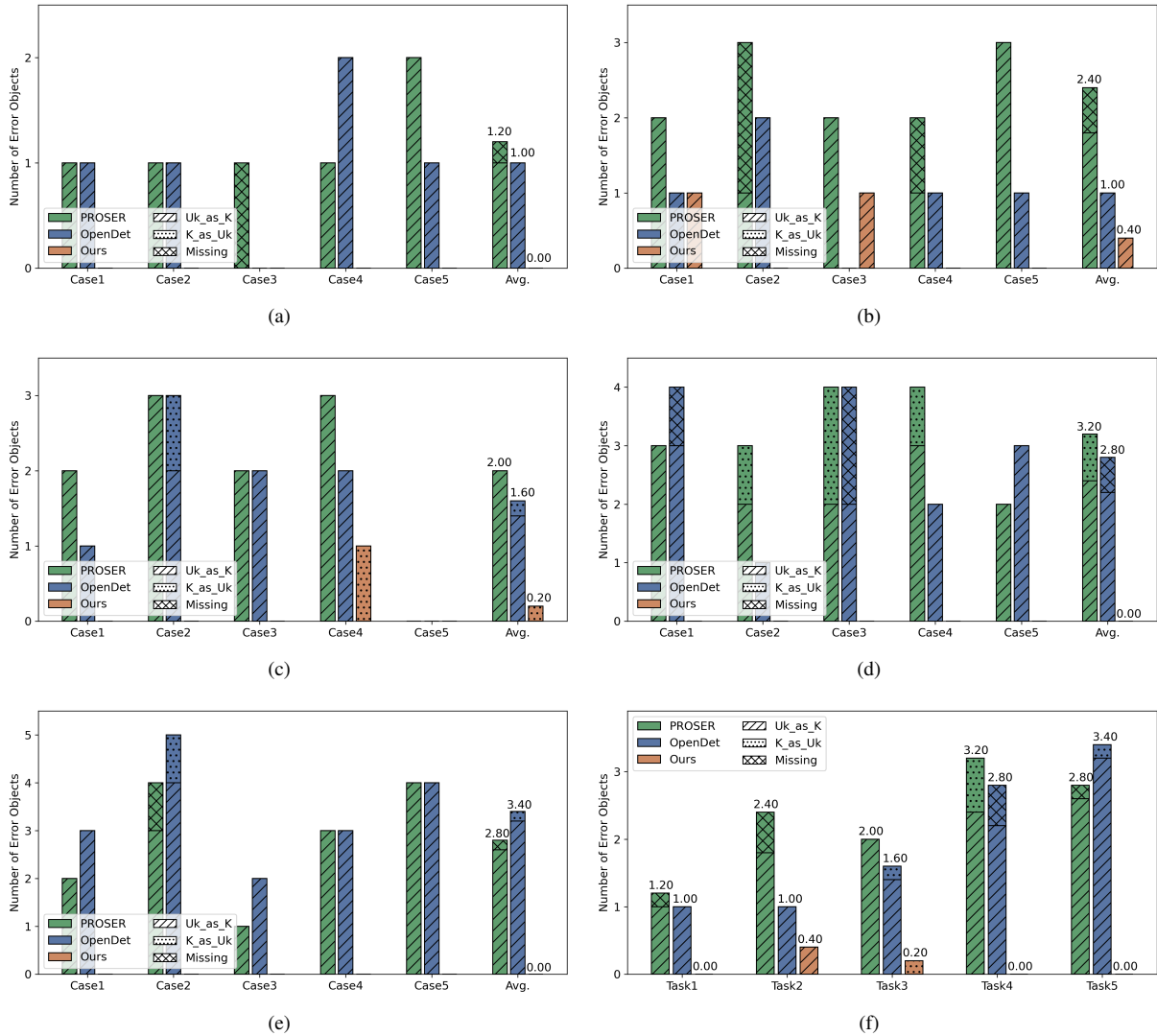


Fig. 14. Comparison of the number of objects wrongly detected. Uk\_as\_K means unknown objects are detected as one of the known categories. K\_as\_Uk means known objects are detected as unknown and Missing means objects are detected as background. (a) The number of wrongly detected objects in Task1, (b) The number of wrongly detected objects in Task2, (c) The number of wrongly detected objects in Task3, (d) The number of wrongly detected objects in Task4, (e) The number of wrongly detected objects in Task5, (f) Average of the number of wrongly detected objects in on 5 tasks.